Degradation of the Formamidinium Cation and the Quantification of the Formamidinium–Methylammonium Ratio in Lead Iodide Hybrid Perovskites by Nuclear Magnetic Resonance Spectroscopy

Peer-reviewed author version

VAN GOMPEL, Wouter; HERCKENS, Roald; REEKMANS, Gunter; RUTTENS, Bart; D'HAEN, Jan; ADRIAENSENS, Peter; LUTSEN, Laurence & VANDERZANDE, Dirk

(2018) Degradation of the Formamidinium Cation and the Quantification of the Formamidinium–Methylammonium Ratio in Lead Iodide Hybrid Perovskites by Nuclear Magnetic Resonance Spectroscopy. In: The Journal of Physical Chemistry C, 112 (8), p. 4117-4124.

DOI: 10.1021/acs.jpcc.7b09805
Handle: http://hdl.handle.net/1942/25874

Degradation of the Formamidinium Cation and the Quantification of the Formamidinium-Methylammonium Ratio in Lead Iodide Hybrid Perovskites by Nuclear Magnetic Resonance Spectroscopy

Wouter T.M. Van Gompel[#,†], Roald Herckens[#,†], Gunter Reekmans[‡], Bart Ruttens[§], Jan D'Haen[§,∥], Peter Adriaensens[‡,§], Laurence Lutsen[§], Dirk Vanderzande[†,§]*

[†]Organic and Bio-Polymer Chemistry, Institute for Materials Research (IMO), Hasselt University, Agoralaan 1-Building D, 3590 Diepenbeek, Belgium

[§]IMOMEC Division, IMEC, Wetenschapspark 1, 3590 Diepenbeek, Belgium

[‡]Research Group of Applied and Analytical Chemistry, Hasselt University, Agoralaan 1-Building D, 3590 Diepenbeek, Belgium

[∥]Material Physics Division, Institute for Materials Research (IMO), Hasselt University, Wetenschapspark 1, 3590 Diepenbeek, Belgium

ABSTRACT

The highest efficiency in perovskite solar cells is currently achieved with mixed-cation hybrid perovskites. The ratio in which the cations are present in the perovskite structure has an important effect on the optical properties and the stability of these materials. At present, the formamidinium cation is an integral part of many of the highest efficiency perovskite systems. In this work, we introduce a nuclear magnetic resonance (NMR) spectroscopy protocol for the identification and differentiation of mixed perovskite phases and of a secondary phase due to formamidinium degradation. The influence of the cooling rate used in a precipitation method on the FA/MA ratio in formamidinium-methylammonium lead iodide perovskites ($FA_xMA_{1-x}PbI_3$) was investigated and compared to the FA/MA ratio in thin-films. In order to obtain the FA/MA ratio from fast and accessible liquid-state ^{1}H-NMR spectra, the influence of the acidity of the solution on the linewidth of the resonances was elucidated. The ratio of the organic cations incorporated into the perovskite structure could be reliably quantified in the presence of the secondary phase through a combination of liquid-state ^{1}H-NMR and solid-state ^{13}C-NMR spectroscopic analysis.

Introduction

Perovskite solar cells currently reach power conversion efficiencies up to 22.1 %.[1,2] Although the original hybrid organic-inorganic perovskite material, methylammonium lead iodide ($CH_3NH_3PbI_3$ or $MAPbI_3$), possesses good optoelectronic properties, the highest solar cell efficiencies are reached using mixed-cation hybrid perovskite systems.[2–6] Additionally, mixed-cation hybrid perovskites have been shown to be more stable than the single-cation $MAPbI_3$, formamidinium iodide ($(NH_2CHNH_2)PbI_3$ or $FAPbI_3$) and cesium iodide ($CsPbI_3$) materials.[3,4] The ratio in which the cations are present in the perovskite material has a significant influence on the optical properties as well as on the stability of the material.[3–6] Therefore, it is important to be able to reliably quantify the relative amounts of the organic cations. Nuclear magnetic resonance (NMR) spectroscopy is ideally suited for this purpose, since it is sensitive to the chemical environment of a variety of nuclei present in hybrid perovskites, such as ^{1}H, ^{13}C, ^{14}N, ^{127}I and ^{207}Pb.[7–13] There has also been recent interest to study mixed-cation hybrid perovskites using NMR spectroscopy. Weber *et al*.[14] and Pisanu *et al*.[15] respectively used liquid-state ^{1}H- and solid-state ^{1}H-NMR spectroscopy to quantify the FA/MA ratio in perovskite powders. More recently, Kubicki *et al*. used a combination of solid-state ^{1}H-, ^{2}H-, ^{13}C-, and ^{14}N-NMR spectroscopy to study the reorientation dynamics of FA and MA cations in hybrid perovskites.[16]

With our work, a spectroscopic protocol towards the identification and differentiation of mixed perovskite phases and a secondary phase due to formamidinium degradation is introduced using a combination of liquid-state ^{1}H-NMR and solid-state ^{13}C-NMR spectroscopy techniques. Using this protocol, quantification of the ratio of organic cations present in the mixed hybrid perovskites was achieved. We noted in liquid-state ^{1}H-NMR spectra, that the linewidth of resonances

corresponding to exchangeable protons (H-N) was dependent on the sample and on the sample preparation. Therefore, we elucidated the underlying factors influencing the linewidth and developed a procedure to consistently obtain resolved liquid-state ^{1}H-NMR spectra for these systems. The necessity for such resolved spectra is illustrated by the ability to detect the presence of ammonium (NH_4^+) as a degradation product in the $FA_xMA_{1-x}PbI_3$ powder samples. The presence of ammonium is related to the degradation of the formamidinium cation in acidic solutions at elevated temperatures, conditions present during a commonly used[14,15,17,18] precipitation synthesis of hybrid perovskite powders. Next to this, the longitudinal relaxation time constant of ^{13}C (T_{1C}) is introduced as a means to differentiate the methylammonium iodide and the formamidinium iodide precursor salts from the mixed perovskite phases using NMR spectroscopy.

Experimental section

Chemicals and reagents

Formamidinium iodide (FAI, > 99.5 %) and lead iodide (PbI_2, 99.999 %) were obtained from Lumtec and used without further purification. Lead acetate trihydrate ($PbAc_2.3H_2O$, 99.995 %) and methylamine (MA, 40 % w/w aq.) were obtained from Alfa Aesar and used without further purification. Hydroiodic acid (HI, 57 % w/w aq., distilled, unstabilized) was purchased from Acros Organics and was used as received. The ammonium iodide (> 99.5 %) was obtained from Merck. The dry dimethylformamide (DMF) that was used was obtained from our in-house solvent-purification system (MBRAUN SPS-800).

Materials preparation

Methylammonium iodide (MAI) was synthesized by neutralizing equimolar amounts of hydroiodic acid (HI, 57 % w/w) and methylamine (40 % w/w) at 0 °C in an ice bath. A precipitate was obtained by evaporation of the solvent using rotary evaporation at 70 °C under reduced pressure. The resulting precipitate was recrystallized three times from ethanol, washed with diethylether; and dried overnight under reduced pressure at room temperature.

For the deposition of mixed formamidinium-methylammonium lead iodide ($FA_xMA_{1-x}PbI_3$) films, precursor solutions were prepared by dissolving lead iodide in water-free DMF at a concentration of 1 mol/L, and adding FAI and MAI to this solution with a combined concentration of 1 mol/L to achieve the desired molar ratio of formamidinium to methylammonium. The precursor solutions were drop-cast onto a large glass plate (20 cm x 10 cm). Prior to deposition, the glass plates were cleaned using deionized water, acetone, and iso-propanol consecutively and subjected to UV-ozone treatment for 60 min at 80 °C. The films were annealed for 30 min at 130 °C on a hot-plate. Powders were obtained from the drop-cast films by scraping the films from the glass plates immediately after they were allowed to cool to room temperature.

$FA_xMA_{1-x}PbI_3$ powders were also prepared using a precipitation synthesis adapted from the method originally reported by Poglitsch and Weber.[17,18] 2.5 g of lead acetate trihydrate was dissolved in 10 mL of hydroiodic acid (57 % w/w) and heated to 100 °C in an oil bath. The flask was flushed with nitrogen gas and kept under a nitrogen atmosphere during the synthesis. Separately, $7.69 \times x$ millimoles of FAI salt together with $7.69 \times (1 - x)$ millimoles of MAI salt were dissolved in 2 mL of deionized water at room temperature. The mixed salt solution was then added dropwise to the lead acetate mixture at 100 °C while stirring. The flask was cooled from

100 °C to 46 °C over a period of 8 hours, unless otherwise stated. The precipitate was separated from the mother liquor through filtration and washed using dry dichloromethane, a non-solvent for the perovskite materials, to remove potential unreacted precursor materials. The resulting powder was dried overnight under reduced pressure at room temperature. The sample containing 100 mol % of formamidinium ($FAPbI_3$) was heated in an oven at 150 °C for 30 min whilst packed in the NMR rotor to convert the material from its hexagonal non-perovskite (delta) phase to its cubic perovskite phase (see Figure S3 of the supporting information for temperature-controlled XRD patterns for a $FAPbI_3$ powder subjected to 150 °C for 30 min) and measured immediately after the rotor had cooled down.

NH_4PbI_3 was prepared by dissolving 2.5 g of lead acetate trihydrate in 10 mL of hydroiodic acid (57 % w/w) and heating to 100 °C in an oil bath. The flask was flushed with nitrogen gas and kept under a nitrogen atmosphere during the synthesis. Separately, 0.955 g of NH_4I was dissolved in 2 mL of deionized water at room temperature. The NH_4I solution was then added dropwise to the lead acetate mixture at 100 °C while stirring. The flask was cooled down from 100 °C to 46 °C over a period of 8 hours. The precipitate was separated from the mother liquor and washed using dry dichloromethane. The resulting powder was dried overnight under reduced pressure at room temperature.

All powders were stored in a glovebox (< 0.1 ppm O_2, < 0.1 ppm H_2O) and were only removed from the glovebox for analysis.

Powder x-ray diffraction (XRD)

X-ray diffraction measurements were mostly performed at room temperature on a Bruker D8 Discover diffractometer with CuK_α radiation. The temperature-controlled XRD measurement to

follow the conversion of delta-$FAPbI_3$ to the perovskite phase of $FAPbI_3$ was carried out in a temperature chamber under a nitrogen flow.

Nuclear magnetic resonance spectroscopy

Liquid-state ^{1}H-NMR spectroscopy measurements

Proton nuclear magnetic resonance spectra of solutions in $(CD_3)_2SO$ (DMSO-d_6) were recorded at room temperature on an Agilent/Varian Inova 400 spectrometer using a 5 mm OneNMR Pulsed-Field-Gradient (PFG) probe. The chemical shift scale (δ; in ppm) was calibrated relative to the residual proton signals of the deuterated solvent (2.5 ppm). Spectra were acquired with a 90° pulse of 6.90 µs, a spectral width of 6.4 kHz, an acquisition time of 4 s, a preparation delay (recycle delay) of 12 s (more than 5 times the longest T_{1H}) and 128 accumulations. The free induction decays are zero-filled to 65 K points and multiplied by a 0.2 Hz exponential line-broadening function prior to Fourier transformation to the frequency domain. The samples were prepared by dissolving 5 mg of perovskite powder in 750 µl of DMSO-d_6 (Euriso-top, D010ES, < 0.02% water content). Details of the calculation of the FA/MA ratio using liquid-state ^{1}H-NMR are explained in the supporting information (Figure S2).

Solid-state ^{13}C-NMR spectroscopy measurements

Solid-state carbon-13 magic angle spinning (MAS) NMR spectra were acquired on an Agilent VNMRS DirectDrive 400MHz spectrometer (9.4 T wide bore magnet) equipped with a T3HX 3.2 mm probe dedicated to small sample volumes and high decoupling powers. MAS was performed at 10 kHz in ceramic rotors of 3.2 mm (22 µl). The aromatic signal of hexamethylbenzene was used to calibrate the carbon chemical shift scale (132.1 ppm). Acquisition parameters used for the spectra and T_{1C} measurements were: a spectral width of 50 kHz, a 90° pulse length of 2.5 µs, an

acquisition time of 30 ms, a recycle delay time of 60 s, a line-broadening of 100 Hz and 1000-2000 accumulations. High power proton dipolar decoupling was set to 50 kHz during the acquisition time. Cross-polarization was not used. The T_{1C} relaxation decay times were measured by the inversion recovery method. The signal intensities were analyzed mono-exponentially as a function of the variable inversion time t according to:

$$I(t) = I_0 \times (1 - 2 \times \exp(-t/T_{1C})) + c^{te}$$

The experimental data were analyzed by a non-linear least-squares fit (Levenberg-Marquardt algorithm).

Results and Discussion

Powder x-ray diffraction of $FA_xMA_{1-x}PbI_3$ powders

Powder X-ray diffraction patterns were obtained to verify the phase purity of the powders, in combination with solid-state NMR spectroscopy. At room temperature the $MAPbI_3$ perovskite adopts a tetragonal phase, with characteristic peak splitting compared to the cubic phase[14], as can be seen in Figure 1. Upon addition of > 10 mol% of FA, the $FA_xMA_{1-x}PbI_3$ system is known to adopt a cubic symmetry[14] and indeed splitting of the reflections is not observed for $x > 10$. No crystalline impurity phases can be identified.

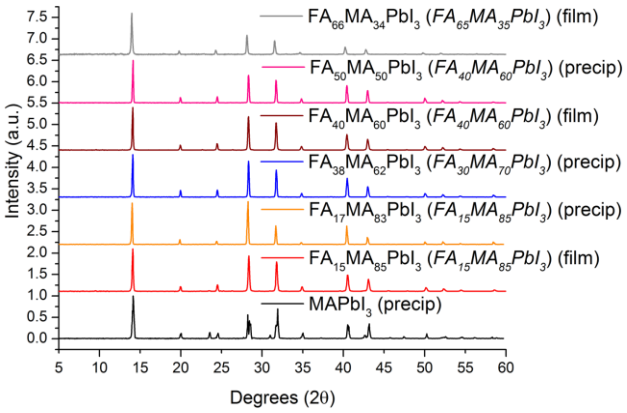

Figure 1 Powder XRD patterns of $FA_xMA_{1-x}PbI_3$ powders. The compositions written between brackets in italics are the nominal compositions. (precip) indicates that the powder was obtained using the precipitation synthesis (cooling rate ~ 6.75 °C/h), (film) indicates that the powder was obtained from scraping off films.

Comparison of sample preparation methods: precipitation vs film

It was observed that the nominal FA/MA ratio (as added in solution) differs from the actual ratio present in the powders prepared using the precipitation method, with an excess of FA being present in the powders (Table 1). This result is in line with the findings described in a recent article by Pisanu *et al*. using the same precipitation method, where the FA/MA ratio was quantified using the deconvolution of solid-state ^{1}H-NMR spectra.[15] The excess FA incorporation was attributed to the difference in solubility and/or reactivity of formamidinium and methylammonium in the precipitation synthesis. This result however differs from the earlier findings of Weber *et al*., who also used this precipitation method to obtain $FA_xMA_{1-x}PbI_3$ powders (the FA/MA ratio was quantified using liquid-state ^{1}H-NMR spectroscopy), but their analysis indicated that the FA/MA ratio in their powders corresponds to the nominal ratio.[14]

Table 1. Nominal and Actual FA/MA Ratio in Powders Obtained Using the Precipitation Method.

Nominal FA/MA ratio	Actual FA/MA ratio as extracted from liquid-state ^{1}H-NMR[a]	Actual FA/MA ratio as extracted from solid-state ^{13}C-NMR[b]
15/85	18/82	17/83
30/70	38/62	38/62
40/60	50/50	50/50

[a] The uncertainty on the FA/MA ratio obtained by liquid-state ^{1}H-NMR is ~ 0.2 %. [b] The uncertainty on the ratio obtained by solid-state ^{13}C-NMR is ~ 1 %.

A difference between the method of Pisanu *et al*., the method of Weber *et al*., and our method is the cooling rate used in the precipitation synthesis. If the reactivity of the two cations is different, it is plausible that the cooling rate influences the ratio in which the cations are incorporated into the mixed perovskite material. Pisanu *et al*. applied a fast cooling rate of 60 °C/h.[15] We reproduced this fast cooling rate, which indeed resulted in a powder with a significant excess of FA compared to the nominal ratio ($FA_{42}MA_{58}PbI_3$ was obtained for a nominal FA/MA ratio of 30/70) (Figure S14). The cooling rate used by Weber *et al*. is not explicitly stated in their article, other than being described as "a gradual lowering of the temperature".[14] In our standard method a cooling rate of ~ 6.75 °C/h was used. A slower cooling rate was also applied to verify if the cooling rate influences the relative incorporation of the cations, since both our study and Pisanu *et al*. find that FA is incorporated in excess to MA. As such, a cooling rate of ~ 1.125 °C/h was also tested (cooling from 100 °C to 46 °C over a period of 48 h). Based on quantification using liquid-state ^{1}H- and solid-state ^{13}C-NMR spectroscopy, an actual FA/MA ratio of 45/55 was obtained in the powder using a nominal ratio of 40/60 (as opposed to the 50/50 ratio obtained using the faster cooling rate

of ~ 6.75 °C/h, Table 1). However, in the X-ray diffraction pattern (Figure 2) of this powder, additional reflections unrelated to the perovskite structure are present, indicative of a secondary crystalline phase being formed during the precipitation synthesis using this slower cooling rate (contrary to samples obtained using the faster cooling rate (Figure 1), which only contain reflections corresponding to perovskite). In the solid-state ^{13}C-NMR spectrum (Figure 3) only resonances corresponding to FA and MA in the perovskite could be identified, indicating that the secondary phase does not contain carbon atoms. Therefore, liquid-state ^{1}H-NMR spectroscopy was applied to elucidate this question and a detailed analysis demonstrated the presence of ammonium (*vide infra*). Degradation of formamidine to ammonia has been described by Stoumpos *et al*.,[19] who observed the presence of needles of $NH_4PbI_3.2H_2O$ being formed together with $FAPbI_3$ during a precipitation synthesis. Formamidine degrades to ammonia and *sym*-triazine ($C_3H_3N_3$) in strongly acidic media (such as hydroiodic acid) at elevated temperatures. A mechanism for this degradation was originally described by Schaefer *et al*.[20] as successive condensation reactions of formamidine, with the release of ammonia during each condensation, leading to a linear trimeric form which cyclizes to the *sym*-triazine molecule (Figure S4). With this knowledge, the degradation product present in the mixture obtained using the slow cooling method was identified using X-ray diffraction as ammonium lead iodide[21,22] (NH_4PbI_3) instead of the dihydrate[23] ($NH_4PbI_3.2H_2O$) as reported by Stoumpos *et al*.[19] (Figure 2). Stoumpos *et al*. cooled their solutions containing the precipitates to room temperature, while we removed our precipitates from the mother liquor at 46 °C. It is known that hydrate formation of crystals of $MAPbI_3$ occurs when cooling the solution below 40 °C using this precipitation method,[17] hence it is plausible that the temperature at which the NH_4PbI_3 crystals are kept in the solution also affects their hydration.

In summary, the reason that a powder with an FA/MA ratio closer to the nominal composition is obtained using slower cooling is probably related to the degradation of FA to NH_3 during the precipitation reaction, since FA was subjected to elevated temperatures in an acidic medium for a much longer time compared to the faster cooling. Likely, the degradation of some of the FA to NH_3 partially compensated for the over-incorporation of FA that we observe when using this precipitation synthesis. It is therefore plausible that powders with the desired FA/MA ratio can be obtained through this method by adding less than the stoichiometric amount of FA to the initial mixture and using a high cooling rate to prevent FA degradation.

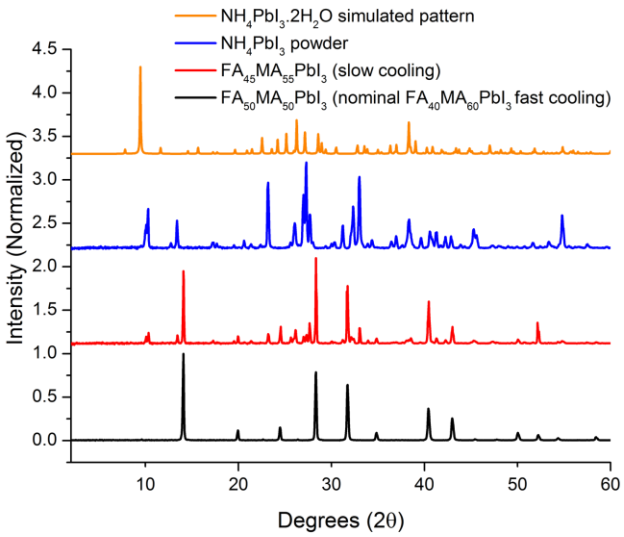

Figure 2. Experimental powder XRD patterns for $FA_{50}MA_{50}PbI_3$ powder (nominal $FA_{40}MA_{60}PbI_3$) obtained using fast cooling (black), the mixture of $FA_{45}MA_{55}PbI_3$ (nominal $FA_{40}MA_{60}PbI_3$) with NH_4PbI_3 obtained using slow cooling (red) and synthesized NH_4PbI_3 powder (blue), and a simulated powder XRD pattern for $NH_4PbI_3.2H_2O$ based on single-crystal XRD data obtained from ref.[23] (orange).

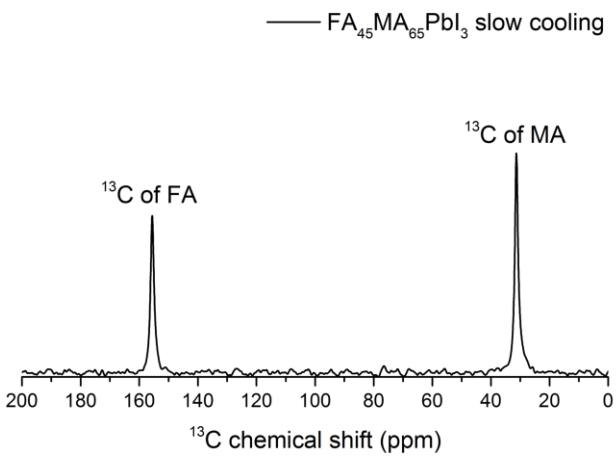

Figure 3. Solid-state ^{13}C-NMR spectrum of $FA_{45}MA_{55}PbI_3$ powder obtained using slow cooling (~1.125 °C/h).

In the powders obtained from thin films, the actual FA/MA ratio is very close to the nominal ratio (Table 2) and only very small amounts of ammonium are present (Figure S8). This indicates that in this case none of the organic components degrades or volatilizes during the deposition and annealing of the thin films. A very small amount of ammonium (~ 0.0075 mol NH_4^+/mol FA) is already present in the commercial formamidinium iodide precursor salt (Figure S8), likely as a residue of the synthesis of formamidine starting from ammonia. Hence, the very small amount of ammonium in the powder samples obtained from the thin films most probably originates from the ammonium present in the FAI precursor salt that was used to prepare the precursor solutions.

Table 2. Nominal and Actual FA/MA Ratio in Powders Obtained from Films.

Nominal FA/MA ratio	Actual FA/MA ratio as extracted from liquid-state ^{1}H-NMR[a]	Actual FA/MA ratio as extracted from solid-state ^{13}C-NMR[b]
15/85	15/85	15/85
40/60	40/60	40/60
65/35	65/35	64/36

[b] The uncertainty on the FA/MA ratio obtained by liquid-state ^{1}H-NMR is ~ 0.2 %. [b] The uncertainty on the ratio obtained by solid-state ^{13}C-NMR is ~ 1 %.

A protocol towards resolved liquid-state ^{1}H-NMR spectra to study mixed-cation hybrid perovskites

The main advantage of liquid-state ^{1}H-NMR is the relatively high sensitivity. As a consequence, only a relatively small amount of material is required to obtain resolved spectra (for our experiments 5 mg of perovskite powder was used for each NMR sample). Additionally, the measuring time is also relatively short, with high-quality spectra being obtained after approximately 30 min for all samples. Finally, liquid-state ^{1}H-NMR spectroscopy is a readily accessible technique for many researchers, therefore, elucidating which factors influence the linewidth of the resonances in spectra of hybrid perovskites is of high relevance to the perovskite research community.

A procedure was developed to attain highly resolved NMR spectra, in which the acidity of the solution plays a crucial role. The procedure is illustrated using a $FA_{38}MA_{62}PbI_3$ (nominal $FA_{30}MA_{70}PbI_3$) powder, obtained using the precipitation method with a cooling rate of ~ 6.75 °C/h as a representative sample. As one can see in Figure 4, when regular DMSO-d_6 is used, the

resonances belonging to the protons bound to nitrogen atoms (exchangeable protons) are not fully resolved (see Figure S5, Figure S6 and Figure S7 of the supporting information for the spectra of the other compositions using regular DMSO-d_6). Hybrid perovskite samples invariably contain exchangeable protons in the form of the protons belonging to the amine and ammonium groups, which can be in exchange with each other and with protons from water present in the solution. This exchange leads to broadening of the resonances, such that the signals belonging to the different groups are not resolved. Furthermore, other resonances (such as NH_4^+, *vide infra*) might be hidden under these broad unresolved bands.

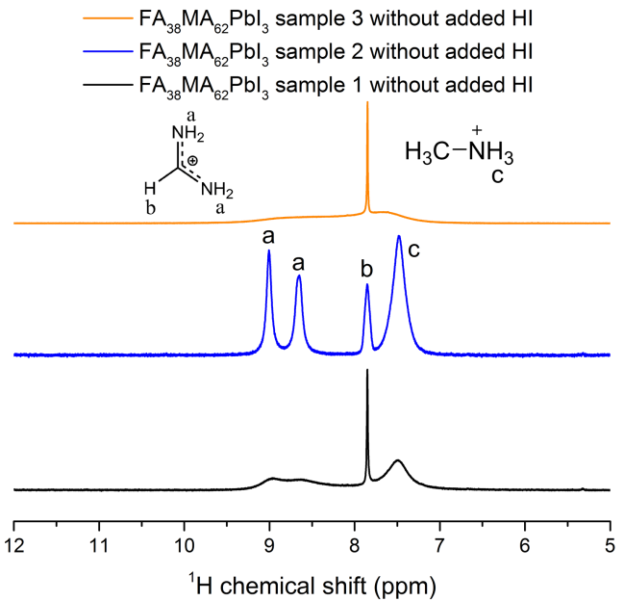

Figure 4 Liquid-state ^{1}H-NMR spectra of $FA_{38}MA_{62}PbI_3$ precipitate powder in DMSO-d_6 without adding hydroiodic acid (HI); three different samplings from the same powder batch. (a) Protons of the FA amine groups (partially positively charged due to resonance) which are not equivalent due to hindered rotation around the partially double bonds (see also Figure S1), (b) CH of FA, (c) NH_3^+ of MA.

Upon measuring NMR spectra of different samplings (of 5 mg each) from the same powder batch, it was noticed that the linewidth of the signals belonging to the exchangeable protons was sample-dependent (Figure 4, for a detailed assignment of the different resonances see Figure S1). Since the NMR samples (Figure 4) were measured immediately after preparation, it is improbable that there was a significant difference in the amount of water present in the NMR solvent for the different samplings (e.g. due to water-ingress through the cap of the NMR tubes). Therefore, another variable should influence the linewidth of these resonances. Since the precipitates are synthesized in the presence of hydroiodic acid (HI), it is plausible that small amounts of HI (distributed inhomogeneously over the powder batch) could still be present in these samples even after washing the precipitates, which in turn could influence the linewidth of the resonances in the spectrum. To test this hypothesis, the NMR samples were spiked with a small amount of hydroiodic acid (1 µl of 57 % w/w HI in 750 µl of DMSO-d_6). This consistently resulted in resolved spectra (Figure 5 and Figure 6), such that the splitting due to ^{1}H-^{1}H coupling could clearly be observed (See Figure S8, Figure S9 and Figure S10 for the spectra of other compositions using DMSO-d_6 spiked with HI, see Figure S1 for an enlarged spectrum and details on the coupling patterns). One also notices that the position of the "water peak" in d_6-DMSO is shifted from the regular positon of ~ 3.33 ppm to ~ 3.70 ppm (Figure 6). The water peak lies between ~ 3.67 ppm and ~ 3.80 ppm for all the samples spiked with HI (Figure S9). The shift occurs towards higher ppm, corresponding to a deshielding effect, which indicates that the electron density around the protons of the water molecules is reduced, which can be related to the formation of H_3O^+. To test if less HI could be added to still obtain resolved spectra, 1 µl of 1/10 diluted HI (starting from 57% w/w) was added to a solution of $FA_{38}MA_{62}PbI_3$ powder (Figure S13). The resonances remain

clearly broadened compared to the spectra with 1 µl of undiluted HI and the splitting due to ^{1}H-^{1}H coupling was no longer observed. Furthermore, the water peak was shifted back to ~ 3.34 ppm.

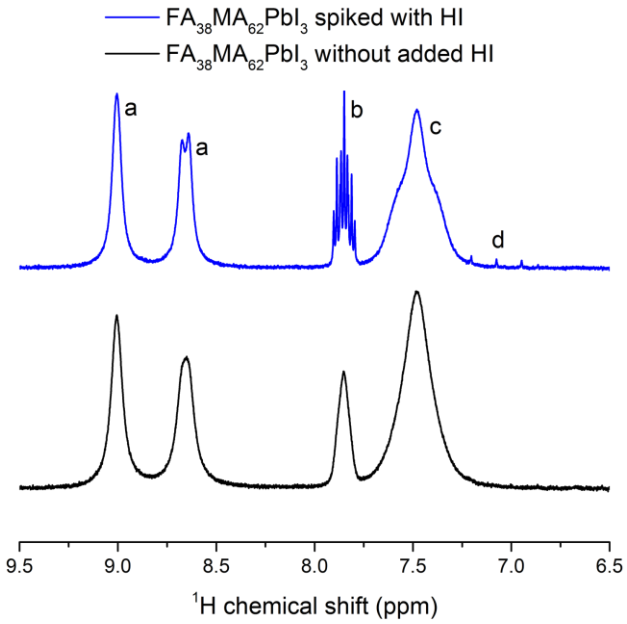

Figure 5. Liquid-state ^{1}H-NMR spectra of $FA_{38}MA_{62}PbI_3$ powder dissolved in DMSO-d_6 spiked with HI (1 µl/750 µl) (top) and without added HI (bottom), showing the region between 6.5 ppm and 9.5 ppm. (a) Protons of the FA amine groups (partially positively charged due to resonance) which are not equivalent due to hindered rotation around the partially double bonds (see also Figure S1), (b) CH of FA, (c) NH_3^+ of MA, (d) NH_4^+.

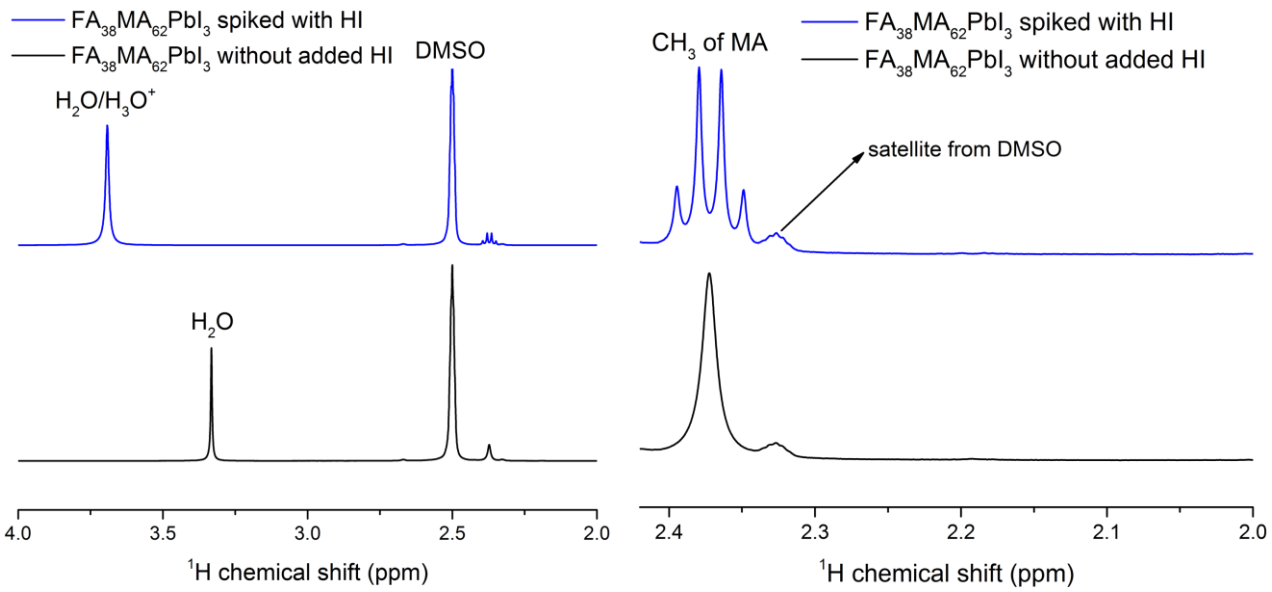

Figure 6. Liquid-state ^{1}H-NMR spectra of $FA_{38}MA_{62}PbI_3$ powder dissolved in DMSO-d_6 spiked with HI (1 µl/750 µl) (top) and without added HI (bottom), showing the region between 4 ppm and 2 ppm (left) and the region between 2.4 ppm and 2 ppm (right).

The importance of obtaining highly resolved spectra is illustrated when analyzing the sample prepared using a slower cooling rate (~1.125 °C/h). As discussed earlier, formamidine degrades to ammonia (NH_3) over time in an acidic medium (HI) at elevated temperatures resulting in the formation of NH_4PbI_3 during the precipitation synthesis. A signal related to the protons of ammonium (NH_4^+) should therefore be present in the liquid-state ^{1}H-NMR spectrum. Nonetheless, no such signal seems to be present at first sight in spectra obtained without added HI (Figure S12). However, when these signals are integrated, one notices that the resonances of the methyl (CH_3) group and the ammonium (NH_3^+) group of methylammonium yield a different value. While both should integrate for three protons, the ammonium group signal integrates for more than three protons (~ 4.3 protons). This indicates that a second resonance overlaps with the resonance of the ammonium group of MA. Upon the addition of HI, three equidistant signals at 7.20, 7.08 and 6.96 ppm can be distinguished next to the resonance corresponding to the NH_3^+ protons of MA at 7.48

ppm. These equidistant signals (Figure 7), which each integrate for the same amount of protons, arise due to the ^{1}H-^{14}N J-coupling ($J_{^{1}H-^{14}N}$ ~ 51 Hz; ^{14}N is a spin-1 nucleus) in NH_4^+ (integrating for a total of ~ 42.41 × 3 = ~ 127, with the CH of FA integrating for 83.25 this gives ~ 0.38 mol NH_4^+/mol FA in this powder obtained *via* slow cooling; see Figure S2 for the integration values). This was verified by dissolving NH_4PbI_3 in DMSO-d_6 spiked with HI. The resulting spectrum indeed matches with a 1:1:1 signal with the same *J*-coupling and the same chemical shift (Figure S11).

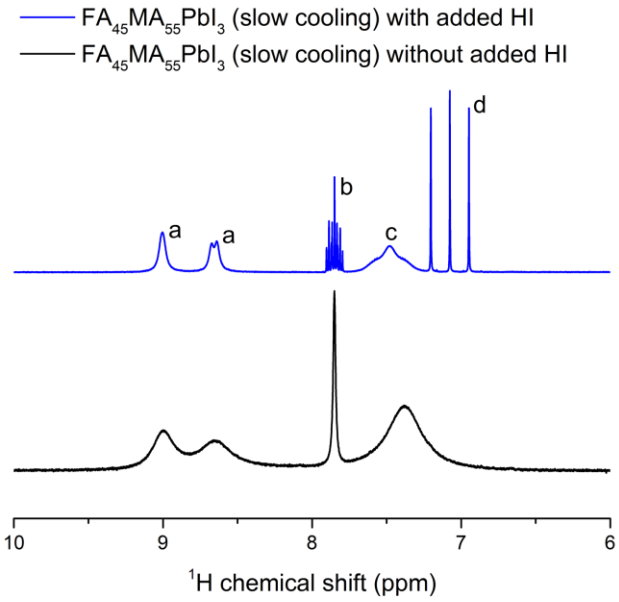

Figure 7. Liquid-state ^{1}H-NMR spectra of $FA_{45}MA_{55}PbI_3$ powder (slow cooled) powder dissolved in DMSO-d_6 spiked with HI (1 µl/750 µl) (top) and without added HI (bottom). (a) Protons of the FA amine groups (partially positively charged due to resonance) which are not equivalent due to hindered rotation around the partially double bonds (see also Figure S1), (b) CH of FA, (c) NH_3^+ of MA, (d) NH_4^+.

Determination of the FA/MA ratio and the presence/absence of secondary phases using solid-state ^{13}C- NMR spectroscopy

Although the protocol developed for liquid-state ^{1}H-NMR spectroscopy is successful in reliably quantifying the FA/MA ratio, no structural information can be obtained through this technique. In order to identify the perovskite phases, as well as possible secondary phases, solid-state NMR spectroscopy must be used. Solid-state NMR spectroscopy is highly compatible with XRD, through which the formation of the perovskite structure can be determined and the absence of crystalline secondary phases can be verified. However, solid-state NMR spectroscopy gives more direct evidence for the incorporation of the FA and MA cation since the chemical environment of the NMR-active nuclei (e.g. ^{13}C) of the FA and MA cations in the perovskite structure is probed.

Solid-state ^{13}C magic-angle spinning (MAS) spectroscopy can be used to quantify the FA/MA ratio in $FA_xMA_{1-x}PbI_3$ solid powders and to verify perovskite phase purity. A disadvantage is the longer acquisition time needed (compared to ^{1}H-NMR) to obtain high quality quantitative spectra and the larger amount of material needed to fill the NMR rotor (~ 75 mg for $FA_xMA_{1-x}PbI_3$ powders). For the $FA_xMA_{1-x}PbI_3$ powders, the ^{13}C resonance of MA is located at ~ 31 ppm while the ^{13}C resonance of FA is located at ~ 156 ppm (spectra in Figure 8). The FA/MA ratio can thus be obtained by integrating both resonances. The FA/MA ratio extracted from the ^{13}C MAS spectra is in all cases close to the ratio obtained using the prescribed liquid-state ^{1}H-NMR spectroscopy procedure (Table 1 and Table 2).

Multiple characteristics of the signals present in a NMR spectrum can give information to verify if an organic cation is incorporated in the perovskite material. A pure $MAPbI_3$ powder is indistinguishable in liquid-state ^{1}H-NMR from a powder of $MAPbI_3$ with some remnants of the

MAI precursor salt still present, while both compounds can be readily distinguished using solid-state ^{13}C-NMR spectroscopy. For MA in the MAI precursor salt, the observed ^{13}C resonance is located at ~ 29 ppm (Table 3), the same as reported earlier by Askar *et al*.[11] Consequently, MAI can be distinguished from $MAPbI_3$ using solid-state ^{13}C-NMR spectroscopy based on the chemical shift. However, this does not work for all hybrid perovskite derivatives, as for example the ^{13}C resonance of FA in the FAI precursor salt is located at the same position (~ 156 ppm) as the ^{13}C resonance of FA in $FAPbI_3$. To solve such a complicated situation, the ^{13}C longitudinal (or spin-lattice) relaxation time (T_{1C}) can be used to distinguish between ^{13}C-nuclei of different chemical species. In the case of the formamidinium cation, the T_{1C} relaxation time of the FAI salt (~ 26 s) is significantly longer than the equivalent in the perovskite (~ 12 s). This is similar for the ^{13}C of the MA cation in the MAI precursor salt, where the T_{1C} is also significantly longer (~ 32 s) for the MA cation than in the perovskite (~ 16 s) (Table 3). Spin-lattice relaxation of the carbon nuclei in these solid-state systems could occur via a variety of mechanisms[24,25], including but not limited to local mobility around the ^{13}C nucleus, but an elucidation of the dominating mechanisms is beyond the scope of this study. For our study, the goal is to differentiate between the species on the basis of the spin-lattice relaxation time.

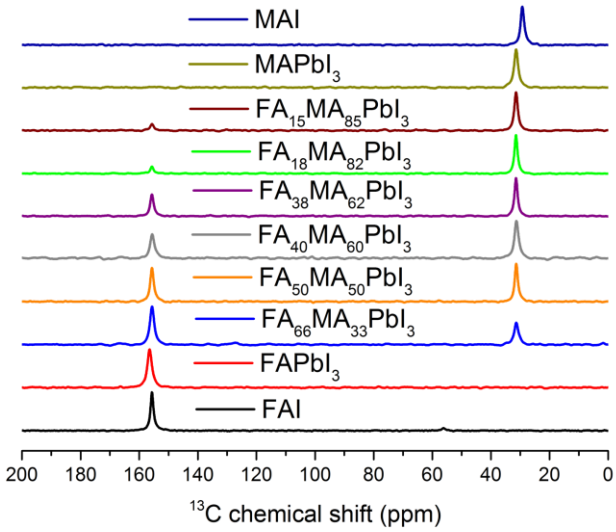

Figure 8. Solid-state MAS ^{13}C-NMR spectra of $FA_xMA_{1-x}PbI_3$ powders and the MAI and FAI precursor salts. Note that for this figure the FA/MA ratio's as obtained from these ^{13}C-NMR spectra are used, as opposed to the ratio's as obtained from liquid-state ^{1}H-NMR spectra that are used for the rest of the figures.

Table 3. Solid-state ^{13}C-NMR Spectroscopy Data of Precursor Salts and $FA_xMA_{1-x}PbI_3$ Phases.

Sample	Method	Nominal FA/MA ratio	Actual FA/MA ratio using solid-state ^{13}C NMR[a]	^{13}C chemical shift FA/MA (ppm)	T_1C FA/MA (s)
MAI	synthesized	-	-	-/29	-/32
FAI	as received	-	-	156/-	26/-
$MAPbI_3$	Precipitation	0/100	0/100	-/31	-/16
$FAPbI_3$ (perovskite phase)	Precipitation	100/0	100/0	156/-	11/-
$FA_{17}MA_{83}PbI_3$	Precipitation	15/85	17/83	156/31	12/16
$FA_{40}MA_{60}PbI_3$	Film	40/60	40/60	156/31	12/16
$FA_{50}MA_{50}PbI_3$	Precipitation	40/60	50/50	156/31	12/16

[a] The uncertainty on the FA/MA ratio obtained by solid-state ^{13}C-NMR is ~ 1 %.

Conclusions

To quantify the FA/MA ratio in $FA_xMA_{1-x}PbI_3$ hybrid perovskite powders in the presence of a secondary phase arising from formamidinium degradation, a combination of liquid-state ^{1}H-NMR spectroscopy and solid-state ^{13}C-NMR spectroscopy was used. The influence of the acidity of the deuterated DMSO solution on the linewidth of resonances belonging to exchangeable protons in liquid-state ^{1}H-NMR spectra was elucidated. Based on this knowledge, a protocol was developed to consistently obtain highly resolved liquid-state ^{1}H-NMR spectra necessary for reliable quantification of $FA_xMA_{1-x}PbI_3$ powders by spiking the solution with hydroiodic acid.

Powders obtained from the precipitation synthesis contained an excess of FA compared to the nominal FA/MA ratio. Lowering of the cooling rate used for the precipitation synthesis resulted in

the degradation of formamidine to ammonia, leading to the formation of ammonium lead iodide as a secondary phase. For the powders obtained from thin-films, the FA/MA ratio was very close to the nominal ratio and no degradation of FA to ammonia occurred.

The NMR spectroscopy techniques that were used are proposed to complement XRD to detect secondary phases in hybrid perovskite systems. It is moreover expected that the procedures presented here can be a guide in the study of other mixed-cation hybrid perovskite systems.

ASSOCIATED CONTENT

Supporting Information

The following files are available free of charge.

Details on the assignment and coupling patterns for liquid-state ^{1}H-NMR spectra of $FA_xMA_{1-x}PbI_3$. Details of the calculation of the FA/MA ratio from liquid-state ^{1}H-NMR spectra, temperature-controlled XRD patterns for $FAPbI_3$, mechanism for the decomposition of formamidine into ammonia and *s*-triazine, liquid-state ^{1}H-NMR spectra for all compositions measured in DMSO-d_6 without HI and in DMSO-d_6 spiked with HI, supporting liquid-state ^{1}H-NMR spectra in relation to the protocol to obtain highly resolved spectra, solid-state ^{13}C- and liquid-state ^{1}H-NMR spectra for a powder obtained using a cooling rate of 60°C/h (like Pisanu et al.[15]). (PDF)

AUTHOR INFORMATION

Corresponding Author

*E-mail: dirk.vanderzande@uhasselt.be. Phone: +32-11-268321

Author Contributions

#These authors contributed equally. The manuscript was written through contributions of all authors. All authors have given approval to the final version of the manuscript.

Notes

The authors declare no competing financial interest.

ACKNOWLEDGMENT

W.V.G. is an SB PhD fellow at FWO (project number 1S17516N), the FWO is acknowledged for the funding of the research. R.H. is a special research fund (BOF) Doctoral (PhD) student at UHasselt/IMO. This work has been carried out in the context of the Solliance network (www.solliance.eu), from which the UHasselt is a full member. Research Foundation Flanders (FWO) and the EU funded network M-ERA.NET are acknowledged for the funding of the PROMISES project.

REFERENCES

(1) National Renewable Energy Laboratory. Best Research-Cell Efficiencies https://www.nrel.gov/pv/assets/images/efficiency-chart.png (accessed Jul 10, 2017).

(2) Yang, W. S.; Park, B.-W.; Jung, E. H.; Jeon, N. J.; Kim, Y. C.; Lee, D. U.; Shin, S. S.; Seo, J.; Kim, E. K.; Noh, J. H.; et al. Iodide Management in Formamidinium-Lead-Halide–based Perovskite Layers for Efficient Solar Cells. *Science* **2017**, *356*, 1376–1379.

(3) Saliba, M.; Matsui, T.; Seo, J.-Y.; Domanski, K.; Correa-Baena, J.-P.; Nazeeruddin, M. K.; Zakeeruddin, S. M.; Tress, W.; Abate, A.; Hagfeldt, A.; et al. Cesium-Containing Triple Cation Perovskite Solar Cells: Improved Stability, Reproducibility and High Efficiency. *Energy Environ. Sci.* **2016**, *9*, 1989–1997.

(4) Jesper Jacobsson, T.; Correa-Baena, J.-P.; Pazoki, M.; Saliba, M.; Schenk, K.; Grätzel, M.; Hagfeldt, A. Exploration of the Compositional Space for Mixed Lead Halogen Perovskites for High Efficiency Solar Cells. *Energy Environ. Sci.* **2016**, *9*, 1706–1724.

(5) Jeon, N. J.; Noh, J. H.; Yang, W. S.; Kim, Y. C.; Ryu, S.; Seo, J.; Seok, S. Il. Compositional Engineering of Perovskite Materials for High-Performance Solar Cells. *Nature* **2015**, *517*, 476–480.

(6) Seo, J.; Noh, J. H.; Seok, S. Il. Rational Strategies for Efficient Perovskite Solar Cells. *Acc. Chem. Res.* **2016**, *49*, 562–572.

(7) Baikie, T.; Barrow, N. S.; Fang, Y.; Keenan, P. J.; Slater, P. R.; Piltz, R. O.; Gutmann, M.; Mhaisalkar, S. G.; White, T. J. A Combined Single Crystal Neutron/X-Ray Diffraction and Solid-State Nuclear Magnetic Resonance Study of the Hybrid Perovskites CH3NH3PbX3 (X = I, Br and Cl). *J. Mater. Chem. A* **2015**, *3*, 9298–9307.

(8) Franssen, W. M. J.; van Es, S. G. D.; Dervişoğlu, R.; de Wijs, G. A.; Kentgens, A. P. M. Symmetry, Dynamics, and Defects in Methylammonium Lead Halide Perovskites. *J. Phys. Chem. Lett.* **2017**, *8*, 61–66.

(9) Roiland, C.; Trippé-Allard, G.; Jemli, K.; Alonso, B.; Ameline, J.; Gautier, R.; Bataille, T.; Le Pollès, L.; Deleporte, E.; Even, J.; et al. Multinuclear NMR as a Tool for Studying Local Order and Dynamics in CH3NH3PbX3 (X = Cl, Br, I) Hybrid Perovskites. *Phys. Chem. Chem. Phys.* **2016**, *18*, 27133–27142.

(10) Rosales, B. A.; Men, L.; Cady, S. D.; Hanrahan, M. P.; Rossini, A. J.; Vela, J. Persistent Dopants and Phase Segregation in Organolead Mixed-Halide Perovskites. *Chem. Mater.*

2016, *28*, 6848–6859.

(11) Askar, A. M.; Bernard, G. M.; Wiltshire, B.; Shankar, K.; Michaelis, V. K. Multinuclear Magnetic Resonance Tracking of Hydro, Thermal, and Hydrothermal Decomposition of CH3NH3PbI3. *J. Phys. Chem. C* **2017**, *121*, 1013–1024.

(12) Senocrate, A.; Moudrakovski, I.; Kim, G. Y.; Yang, T.-Y.; Gregori, G.; Grätzel, M.; Maier, J. The Nature of Ion Conduction in Methylammonium Lead Iodide: A Multimethod Approach. *Angew. Chemie Int. Ed.* **2017**, *56*, 7755–7759.

(13) Levchuk, I.; Hou, Y.; Gruber, M.; Brandl, M.; Herre, P.; Tang, X.; Hoegl, F.; Batentschuk, M.; Osvet, A.; Hock, R.; et al. Deciphering the Role of Impurities in Methylammonium Iodide and Their Impact on the Performance of Perovskite Solar Cells. *Adv. Mater. Interfaces* **2016**, *3*, 1600593.

(14) Weber, O. J.; Charles, B.; Weller, M. T. Phase Behaviour and Composition in the Formamidinium-Methylammonium Hybrid Lead Iodide Perovskite Solid Solution. *J. Mater. Chem. A* **2016**, *4*, 15375–15382.

(15) Pisanu, A.; Ferrara, C.; Quadrelli, P.; Guizzetti, G.; Patrini, M.; Milanese, C.; Tealdi, C.; Malavasi, L. The FA1– xMAxPbI3 System: Correlations among Stoichiometry Control, Crystal Structure, Optical Properties, and Phase Stability. *J. Phys. Chem. C* **2017**, *121*, 8746–8751.

(16) Kubicki, D. J.; Prochowicz, D.; Hofstetter, A.; Péchy, P.; Zakeeruddin, S. M.; Grätzel, M.; Emsley, L. Cation Dynamics in Mixed-Cation (MA)x(FA)1– xPbI3 Hybrid Perovskites from Solid-State NMR. *J. Am. Chem. Soc.* **2017**, *139*, 10055–10061.

(17) Poglitsch, A.; Weber, D. Dynamic Disorder in Methylammoniumtrihalogenoplumbates (II) Observed by Millimeter-wave Spectroscopy. *J. Chem. Phys.* **1987**, *87*, 6373–6378.

(18) Leguy, A. M. A.; Azarhoosh, P.; Alonso, M. I.; Campoy-Quiles, M.; Weber, O. J.; Yao, J.; Bryant, D.; Weller, M. T.; Nelson, J.; Walsh, A.; et al. Experimental and Theoretical Optical Properties of Methylammonium Lead Halide Perovskites. *Nanoscale* **2016**, *8*, 6317–6327.

(19) Stoumpos, C. C.; Malliakas, C. D.; Kanatzidis, M. G. Semiconducting Tin and Lead Iodide Perovskites with Organic Cations: Phase Transitions, High Mobilities, and Near-Infrared Photoluminescent Properties. *Inorg. Chem.* **2013**, *52*, 9019–9038.

(20) Schaefer, F. C.; Hechenbleikner, I.; Peters, G. A.; Wystrach, V. P. Synthesis of the Sym-Triazine System. I. Trimerization and Cotrimerization of Amidines. *J. Am. Chem. Soc.* **1959**, *81*, 1466–1470.

(21) Fan, L.-Q.; Wu, J.-H. NH4PbI3. *Acta Crystallogr. Sect. E Struct. Reports Online* **2007**, *63*, 189– 191.

(22) Zong, Y.; Zhou, Y.; Ju, M.; Garces, H. F.; Krause, A. R.; Ji, F.; Cui, G.; Zeng, X. C.; Padture, N. P.; Pang, S. Thin-Film Transformation of NH4PbI3 to CH3NH3PbI3 Perovskite: A Methylamine-Induced Conversion-Healing Process. *Angew. Chemie Int. Ed.* **2016**, *55*, 14723–14727.

(23) Bedlivy, D.; Mereiter, K. The Structures of Potassium Lead Triiodide Dihydrate and Ammonium Lead Triiodide Dihydrate. *Acta Crystallogr. Sect. B Struct. Crystallogr. Cryst. Chem.* **1980**, *36*, 782–785.

(24) Beckmann, P. A.; Bai, S.; Dybowski, C. ^{111}Cd and ^{113}Cd Spin-Lattice Relaxation in $CdMoO_4$ by Paramagnetic Centers in the Absence of Spin Diffusion. *Phys. Rev. B* **2005**, *71*, 12410.

(25) Taylor, R. E.; Leung, B.; Lake, M. P.; Bouchard, L.-S. Spin–Lattice Relaxation in Bismuth Chalcogenides. *J. Phys. Chem. C* **2012**, *116*, 17300–17305.

TOC Graphic